Seismic Wave Anisotropy in the D" Region and its Implications

Thorne Lay, Quentin Williams

Earth Sciences Department and Institute of Tectonics, University of California, Santa Cruz California

Edward J. Garnero

Department of Geology and Geophysics and Seismological Laboratory, University of California, Berkeley, California

Louise Kellogg

Department of Geology, University of California, Davis, California

Michael E. Wysession

Department of Earth and Planetary Sciences, Washington University, St. Louis, Missouri

Seismological observations provide evidence for localized regions of anisotropic splitting of shear waves that graze through the D" region at the base of mantle. Beneath Alaska and the Caribbean *S*, *Sdiff* (diffracted *S*), and *ScS* phases exhibit shear wave splitting with the longitudinal component (*SV*, in the standard great-circle reference frame) delayed relative to the transverse component (*SH*) by as much as 4-9 s. This can be explained by the presence of 1-3% transverse isotropy (hexagonal symmetry with a vertical axis) within the D" region. These circum-Pacific areas have higher-than-average lower mantle shear velocities as well as localized *S* velocity discontinuities (but no detectable *P* velocity discontinuities) at the top of a 200-300 km thick D" layer. It appears that the anisotropy exists at and below the D" discontinuity, resulting in a stronger velocity contrast for *SH* than for *SV*. The magnitude of anisotropy varies laterally, and can decrease to zero over scale lengths of about 1000 km. Beneath the central Pacific Ocean, where the lowermost mantle appears to have lower-than-average shear velocities, little or no D" discontinuity, and strongly negative velocity gradients within D", there are intermittent observations of *Sdiff*, *S*, and *ScS* splitting with relatively early arrivals on either SH or SV components. The variable splitting suggests the presence of non-vertical hexagonal symmetry axis or general anisotropy in localized patches, apparently concentrated toward the core-mantle boundary.

INTRODUCTION

Determination of the dynamical processes occurring in the thermal and chemical boundary layer at the base of the mantle is of great importance to fundamental geophysical problems such as the nature of mantle convection, the

The Core-Mantle Boundary Region
Geodynamics 28

Various mechanisms for generating anisotropy in D" are considered, including lattice preferred orientation (LPO) of anisotropic minerals in the D" boundary layer, anisotropic structures of slab remnants that have sunk to the base of the mantle, and shape preferred orientation (SPO) induced by shearing of chemical heterogeneities and/or zones of partial melt resulting in horizontally or vertically laminated fabrics. Constraining D" dynamical properties from shear wave anisotropy has potential, but the observational and modeling challenges remain formidable.

process of core formation, and the nature of coupling between the core and mantle [e.g., *Stacey and Loper*, 1983; *Lay*, 1989; *Loper and Lay*, 1995]. Seismological investigations provide the strongest constraints on the core-mantle transition zone, with substantial complexity of the deep elastic velocity structure having been revealed by seismic waves [see reviews by *Young and Lay*, 1987; *Lay*, 1995]. There is much progress in mapping of large-scale patterns of volumetric heterogeneity [e.g., *Su et al.*, 1994; *Li and Romanowicz*, 1996; *Grand et al.*, 1997], with higher velocity regions often accompanied by *P* and *S* velocity discontinuities at the top of the D" region (the lowermost 200-300 km of the mantle) [see *Wysession et al.*, 1998]. There is also evidence for a thin, laterally varying ultra-low velocity zone (ULVZ), with *P* and *S* velocity reductions of 10% or more right above the core-mantle boundary (CMB) [see *Garnero et al.*, 1998]. These seismological investigations suggest the presence of chemical and thermal heterogeneity, and possibly partial melt, in a dynamic boundary layer at the base of the mantle [*Lay et al.*, 1998].

While resolving the elastic *P* and *S* wave velocity structures in D" is an important undertaking, interpretation of isotropic seismological models in terms of boundary layer processes is very poorly constrained. Many trade-offs exist between plausible thermal and chemical contributions to the observed structures, and inferred dynamical processes are correspondingly non-unique; what is needed is a seismic observable more directly influenced by dynamical processes. For lithospheric investigations, observations of anisotropic seismological properties have proved to be significant for dynamic interpretations, because the mineralogical preferred orientation and cracking processes that produce seismic anisotropy in the lithosphere appear to be directly linked to large-scale deformations of the medium [e.g., *Kawasaki*, 1986; *Nataf et al.*, 1986; *Karato*, 1989; *Silver*, 1996]. Anisotropic structures in the asthenosphere are also valuable for inferring mantle processes, although the lack of direct constraint on the flow regime complicates the interpretations [e.g., *Karato*, 1989].

A substantial number of observations are consistent with the presence of laterally varying seismic anisotropy with variable symmetry orientation in the D" region. These seismological observations require geodynamical and mineral physics interpretations. We conduct a multidisciplinary examination of the current status of this topic to provide impetus for further work on a difficult, but promising approach to enhancing our understanding of the dynamical processes in the core-mantle transition zone.

CHALLENGES TO OBSERVING DEEP MANTLE ANISOTROPY

Seismic anisotropy can be detected in *P* wave travel times if extensive raypath coverage is available and if the effects can be localized spatially to a particular region. While this has proved to be the case in some investigations of *Pn* and *P* wave travel time anomalies for studying the crust and uppermost mantle [e.g., *Morris et al.*, 1969; *Dziewonski and Anderson*, 1983], neither criterion can be readily satisfied for studies of the base of the mantle. Anisotropy may arise from fine layering of materials with strong contrasts in physical properties, and the presence of lamination in the deep mantle may possibly be detected by high resolution imaging of velocity structure [e.g., *Weber*, 1994]. However, there are many difficulties in recovering deterministic models for high frequency energy traversing all the way to the D" region. Patterns of small scale heterogeneities that produce scattering of *PKP* phases have led to some speculations on anisotropic fabrics in D" [e.g., *Haddon*, 1982; *Cormier*, 1995], but the models are very poorly resolved and there are strong trade-offs with CMB topography, which at present is poorly known. Seismic anisotropy can also be detected in the behavior of surface waves or free oscillations [e.g., *Nishimura and Forsyth*, 1988; *Tanimoto and Anderson*, 1985], but as yet these waves provide little constraint on anisotropic structure near the CMB. Mantle models need to improve before normal modes can be exploited as they are for the lithosphere. Given the limitations of *P* waves and normal modes, the most effective probe of anisotropic structure in the deep mantle is shear wave splitting.

Shear wave splitting occurs when an *S* wave traverses a seismically anisotropic region, with the *S* wave energy partitioning into two polarizations that propagate with different velocities. The overall polarization of the *S* wave is thus modified, and can be used to infer characteristics of the anisotropic structure. If the path length is known, the magnitude of anisotropy can be inferred from the time shift between the split *S* arrivals, and the orientation can be determined from the polarization angles of the fast and slow waves.

In general, the lower mantle does not exhibit significant shear wave splitting for teleseismic S wave signals [e.g., *Kaneshima and Silver*, 1992; *Meade et al.*, 1995b], despite the intrinsic anisotropy of major lower mantle minerals such as perovskite [e.g., *Mao et al.*, 1991] and periclase, and the likely presence of shear flows associated with upwellings and downwellings. Most observations of shear wave splitting in teleseismic signals have been explained in terms of shallow mantle anisotropy beneath seismic stations and in the vicinity of subducting slabs [e.g., *Silver*, 1996]. Indeed, the upper 100-300 km of the mantle has significant anisotropy that can affect body wave signals that traverse the deep mantle.

The main strategy for identifying shear wave splitting caused by deep mantle anisotropy has been analysis of polarization of S waveforms. Comparisons of S and ScS or SKS and $Sdiff$ (S wave energy diffracted by the core) are made to bound source and receiver contributions to the overall S waveforms and polarization. Recent models of lithospheric anisotropy can account for shallow anisotropic effects explicitly, either by selecting stations that are known to lack lithospheric anisotropy or by correcting for the splitting effects predicted by lithospheric models. However, correction for shallow effects is not an error-free procedure, and several studies [e.g., *Garnero and Lay*, 1997; *Vinnik et al.*, 1998] have found that corrections based on existing models are not always correct; improved lithospheric corrections must be determined. It is always necessary to account for lithospheric anisotropic effects.

For earthquake sources located within subducting slabs one must also consider the possibility that near-source slab structure is anisotropic, as this is expected given the observed anisotropy of oceanic lithosphere [e.g., *Anderson*, 1987; *Kendall and Thomson*, 1993]. In this case, S wave splitting may have complex variations with azimuth and take-off angle with respect to the dipping slab, making it difficult to even detect the near-source effect. Existing anisotropic slab models are inadequate for making corrections, and empirical arguments are usually invoked to rule out near-source contributions; however, none of the studies considered here convincingly eliminate near-source contributions.

Correcting for shallow mantle anisotropy is not the only challenge for quantifying deep mantle anisotropy. Body waves that reach the core-mantle transition zone have long paths through the heterogeneous mantle, and relatively short paths within the D" region, reducing sensitivity to any deep anisotropy. Increasing the proportion of path length within the deep mantle mandates the study of grazing waves, which have much greater sensitivity to the overall velocity structure than do the steeply incident waves used in most studies of lithospheric anisotropy. The depth extent over which D" anisotropy may occur is not known independently, and it is essential to account for the precise raypath when estimating path length within a possibly anisotropic zone [*Garnero and Lay*, 1998]. For core-grazing geometries, distance dependence of anisotropic observations may involve either depth dependence or lateral variations in the anisotropic structure [*Ritsema et al.*, 1998].

Accounting for propagation effects on S wave polarization is also essential. Layered structure imparts distinct effects on longitudinally (SV) and transversely (SH) polarized S wave motions, as defined relative to the vertical plane containing the source and receiver. Differences in the frequency dependent interactions of SV and SH polarizations with the CMB, with radial gradients in the D" region, and with any discontinuities in the medium, add complexity to the S wavefield that will superimpose on any effects of anisotropic splitting. If splitting occurs, the fast and slow polarizations will each have SV and SH components of motion relative to any radial layering that is encountered as the grazing wave turns, possibly obscuring the effects of the splitting. The reflection coefficient for SV and SH components of ScS causes non-linear particle motion at some distances, as does diffraction, even for a standard Earth model lacking strong gradients in D" [e.g., *Maupin*, 1994]. Finally, small-scale lateral heterogeneity of isotropic structure can produce waveform complexity easily misinterpreted as the result of transmission through an anisotropic zone [e.g., *Grechka and McMechan*, 1995]. Indeed, a laminated region with many thin layers of isotropic structure is indistinguishable from a medium with intrinsic mineralogical anisotropy for certain geometries and wavelengths [*Backus*, 1962]. Strong velocity gradients and multi-scale heterogeneity do exist in D" [e.g., *Lay*, 1989] as well as thin layers [e.g., *Garnero and Helmberger*, 1995; *Garnero et al.*, 1993, 1998], thus the observational challenges of quantifying D" anisotropy should not be underestimated.

SEISMOLOGICAL OBSERVATIONS OF ANISOTROPY IN THE D" REGION

The observational challenges noted above have slowed development of anisotropic models for the D" region compared to the more extensive progress in mapping out isotropic structures [see *Wysession et al.*, 1998]. Another factor is that well-calibrated digital broadband instrumentation is particularly valuable for making subtle S wave polarization measurements, and such data have only become abundant in the past decade. There has been a flurry of papers on D" anisotropy in the past 3 years, but these build on important earlier work, which we describe first.

Early studies of shear wave splitting

Systematic waveform differences between S and ScS arrivals in long-period World Wide Standardized Seismograph Network (WWSSN) recordings were first observed by *Mitchell and Helmberger* [1973] and *Lay and Helmberger* [1983b]. $ScSV$ components often have slightly late peaks relative to $ScSH$ components, in contrast to more consistent relative times of S wave components. *Mitchell and*

Helmberger [1973] studied paths beneath the Caribbean, with *ScSV* peaks ranging from 0 to 3 s behind *ScSH*. *Lay and Helmberger* [1983b] extended those observations, and added paths beneath Alaska, where the peak of *ScSV* is sometimes as much as 4 s late relative to *ScSH*. Neither study corrected for shallow mantle anisotropy (due to the lack of obvious *S* splitting), and both performed isotropic waveform modeling, achieving satisfactory fits to the observations by introducing thin (20 to 40 km) high velocity layers (as much as 5% higher than standard values) at the CMB. *SH* and *SV* component interactions with such a thin layer cause an apparent shift of the *ScS* peak on the two components in the long-period WWSSN passband (internal multiples within the layer must be accounted for).

The WWSSN data have a positive 1 s baseline shift (with a ±1 s range of data) in the *ScSV*-*ScSH* observations from 40° to 75° for the Caribbean and Alaskan paths, and the delay of *ScSV* increases rapidly with distance from 75° to 80° beneath Alaska. The rapid increase (but not the baseline shift) can be explained by the thin high velocity layer model. Explanation of the baseline shift and rapid increase in terms of anisotropy requires lateral variation in the magnitude of anisotropy beneath Alaska. *Cormier* [1986] attempted to explain these data with D" models with transverse isotropy (hexagonal symmetry with a vertical symmetry axis, for which the *SV* and *SH* components are not coupled) in a 150 km thick zone with anisotropy increasing with depth to a maximum at the CMB. His synthetics produce phase shifts of the overall *ScS* waveform relative to *S*, but, in detail, do not match the shift of the peaks of *ScSV* and *ScSH* that was previously measured.

Doornbos et al. [1986] sought to reconcile thermal boundary layer models with *P* and *S* wave velocity structures inferred from diffracted waves by invoking transverse isotropy D". However, this approach is predicated on the existence of globally representative velocity structures for D", which is inconsistent with the strong heterogeneity in the region (most published *Sdiff* decay spectra exhibit huge scatter [e.g., *Doornbos and Mondt*, 1979]).

Diffracted wave analysis gained attention with the report of broadband *SVdiff* signals at large distances into the core shadow zone by *Vinnik et al.* [1989]. A few low amplitude longitudinal signals were found near the time of strong tangential *Sdiff* arrivals at distances near 118° for paths bottoming beneath the central Pacific, with a possible 1/4 period phase shift of the *SV* component of the *Sdiff* energy. For Earth models with mild velocity gradients in D" *SV* energy does not diffract efficiently relative to *SH*, predicting that *Sdiff* become predominantly transversely polarized beyond distances of 105°. While noting that a strong negative velocity gradient in D" can allow *SVdiff* energy to propagate further than expected for a standard Earth model [e.g., *Kind and Müller*, 1977], *Vinnik et al.* [1989] invoked azimuthal anisotropy in D" which would couple the *SV* and *SH* energy, allowing strong (quasi-) *SH* diffractions to couple into weak *SV* diffractions. No corrections were made for lithospheric anisotropy in this study, but subsequent correction of the same data by *Maupin* [1994] did not eliminate the non-linear polarization. There is now evidence for a strong negative shear velocity gradient beneath the central Pacific in the distance decay of *SVdiff* energy, and the polarization of *Sdiff* waveforms for corresponding isotropic structures is complicated [*Ritsema et al.*, 1997], thus, interpretation of *SVdiff* observations deep in the shadow zone requires knowledge of the structure in D" along the entire path, which is very difficult to achieve.

Profiles of long-period WWSSN *SV* waveforms were considered by *Lay and Young* [1991], with amplitude and waveform data at distances from 70° to 105° used to estimate D" shear velocity structure beneath Alaska and the northern Pacific. A shear velocity discontinuity exists 200-300 km above the CMB in this region [*Lay and Helmberger*, 1983a; *Young and Lay*, 1990; *Matzel et al.*, 1996], which predicts non-linear *S* wave polarizations in the distance range 90° to 105°. The *SV* amplitudes decay rapidly beyond 95°, consistent with positive, or only slightly negative velocity gradients in D". Some data exhibit shifts in the apparent onset of *SV* and *SH* at distances near 95°, with *SV* being delayed by from 0 to 4.5 s, which cannot be accounted for by isotropic structure. The delayed *SV* arrivals bottom in the same vicinity as the delayed *ScSV* arrivals observed by *Lay and Helmberger* [1983b], but the thin high velocity layer models that had been invoked to explain the latter data do not predict a shift of *S* arrivals near 95°. This suggests that laterally varying anisotropy at the base of the mantle is a more reasonable explanation for both data sets. Application of receiver lithospheric anisotropy corrections to both data sets [*Garnero and Lay*, 1997] supports this conclusion.

Recent studies of shear wave splitting

The studies mentioned above established the basic approaches to detecting lower mantle anisotropy. Recent work has utilized higher quality data sets to examine shear waves in the three key distances ranges (*ScS* at distances from 50° to 80°; *S* grazing D" at distances of from 90 to 105°; and *Sdiff* in the core shadow beyond about 105°). Figure 1 shows a map summarizing the regions that have now been sampled, keyed to Table 1, which identifies associated references and seismic phases analyzed. The map also indicates the nature of the anisotropy detected in each region, characterized by whether the *SH* velocity (Vsh) or for the *SV* velocity (Vsv) is larger. In general, shear wave splitting is most evident when fast and slow quasi-shear wave polarizations are aligned with the great-circle reference frame, but there is no physical requirement that this be the case. Generic raypaths of each of the three principal data types are illustrated in Figure 2. Examples of waveforms exhibiting splitting for each geometry are shown in Figure 3.

Only a small portion of the lowermost mantle has been examined, and recent work has emphasized the same basic regions studied in the early studies discussed above; beneath

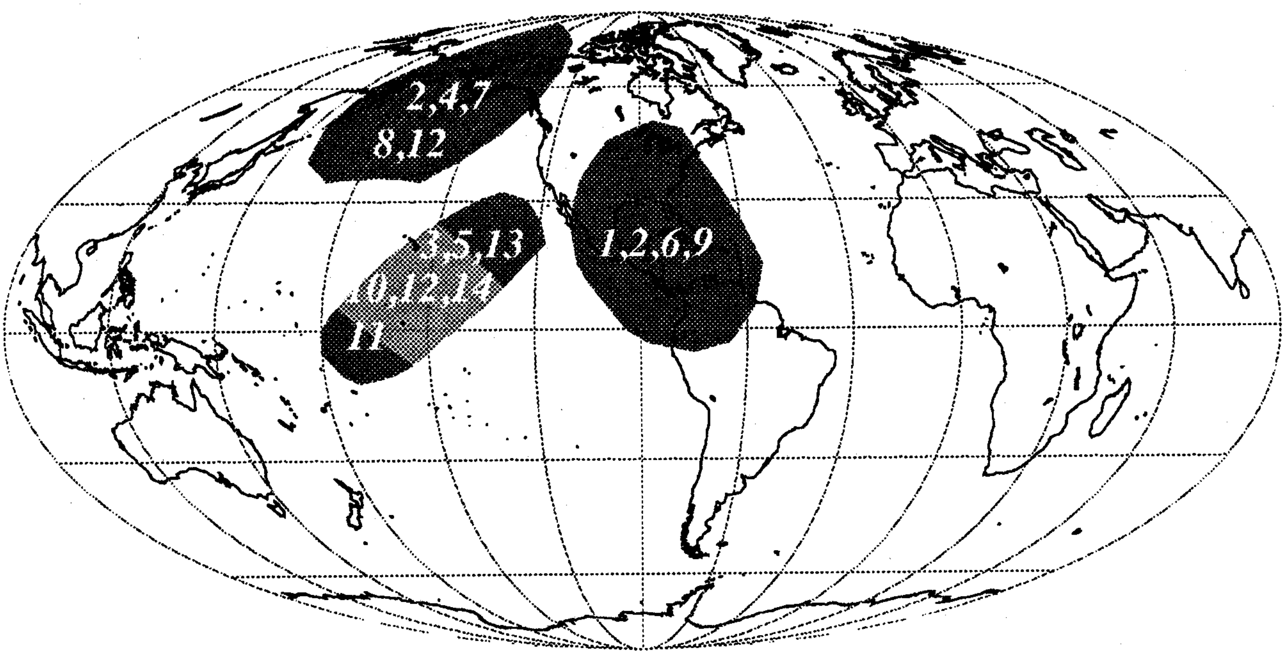

Figure 1. Global map showing regions of D" that have at least some reported evidence of shear wave splitting, with the number indicating the corresponding reference in Table 1. The darker regions under the Caribbean and Alaska are consistent with laterally varying transverse isotropy from 0 to 2%, producing relative early tangential component *S*, *ScS* and *Sdiff* signals. The region under the Pacific has variable anisotropy, with the northeasternmost and southwesternmost areas (darker shading) possibly having transverse isotropy, while the central area (lighter shading) has either no anisotropy or patchy azimuthal anisotropy.

Table 1. Observations of Shear Velocity Anisotropy in D"

No.	Reference	S Phases Used	Sense of Splitting
1	*Mitchell and Helmberger* [1973]	*ScS*	Vsh>Vsv
2	*Lay and Helmberger* [1983b]	*ScS*	Vsh>Vsv
3	*Vinnik et al.* [1989]	*Sdiff*	Azimuthal
4	*Lay and Young* [1991]	*ScS, S*	Vsh>Vsv
5	*Vinnik et al.* [1995]	*Sdiff*	Vsh>Vsv
6	*Kendall and Silver* [1996]	*S*	Vsh>Vsv
7	*Matzel et al.* [1996]	*S*	Vsh>Vsv
8	*Garnero and Lay* [1997]	*ScS, S, Sdiff*	Vsh>Vsv
9	*Ding and Helmberger* [1997]	*ScS*	Vsh>Vsv
10	*Pulliam and Sen* [1998]	*S*	Vsv>Vsh
11	*Vinnik et al.* [1998]	*Sdiff*	Vsh>Vsv
12	*Kendall and Silver* [1998]	*S, Sdiff*	Vsh>Vsv/None
13	*Ritsema et al.* [1998]	*Sdiff*	Vsh>=<Vsv
14	*Russell et al.* [1998]	*ScS*	Vsh>=<Vsv

the Caribbean, Alaska and the Central Pacific. While there is a need to extend the coverage as much as possible, it has been essential to first establish the strength and variability of the anisotropic observations (or lack of anisotropy) in each region with higher quality data and modeling. We summarize recent observations in each of the three regions.

Caribbean. Kendall and Silver [1996] analyzed high quality digital *S* and *Sdiff* waves in the distance range 90° to 110° for paths sampling D" below the Caribbean. They corrected for relatively strong lithospheric anisotropy effects under the Canadian seismic stations used. Delays of 3-9 s in the apparent onset of the *SV* components are consistent with transverse isotropy with a vertical axis, but there is little azimuthal coverage. Absence of splitting of direct *S* waves at closer distances indicates that the anisotropy is located in the deep mantle. The sense of the delay observed by *Kendall and Silver* [1996] is similar to that seen in *ScS* splitting for paths with shorter lengths in D" by *Mitchell and Helmberger* [1973] and *Lay and Helmberger* [1983b] for the same region, but the magnitude is larger, consistent with either an effect that accumulates with distance or possibly a northward increase in the magnitude of anisotropy. *Ding and Helmberger* [1997] show further examples of late *ScSV* in broadband recordings for paths under the Caribbean.

An appropriate reference model is needed to constrain the depth range of anisotropy. The Caribbean region has a laterally varying shear velocity discontinuity about 250±50 km above the CMB [e.g., *Lay and Helmberger*, 1983a; *Kendall and Nangini*, 1996; *Ding and Helmberger*, 1997], which imparts complexity to the *S* waveforms that must be distinguished from anisotropy. *Ding and Helmberger* [1997] note that there is evidence for *SV* reflections from

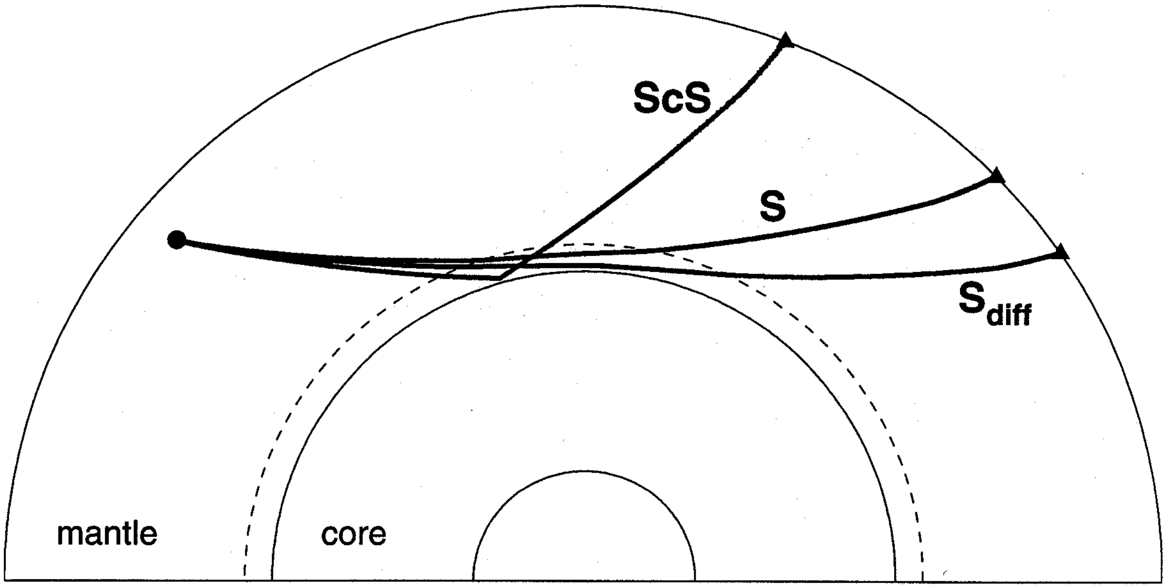

Figure 2. Raypath for the three basic classes of seismic shear wave used to examine anisotropy in the lowermost mantle: *ScS*, *S* near 95° and *Sdiff* in the core shadow zone.

the top of D" under the Caribbean, so the *S* wave discontinuity is not manifested only in Vsh. Any *P* wave discontinuity beneath the Caribbean region is much smaller than the 3% *S* wave discontinuity, and the *P* velocity structure may be smoothly varying with depth. *Ding and Helmberger* [1997] show isotropic broadband *SV* synthetics for distances beyond 90° with strong secondary arrivals caused by energy traveling above the discontinuity, while weak initial motions are associated with energy that actually penetrates into D". If the latter is obscured by noise or weakened by strong attenuation, one could infer an erroneous splitting by comparison of the strong onsets for *SH* and *SV* signals.

At distances of 90°-95° the *SV* arrival sometimes has an initial weak motion which appears to have opposite polarity to what is expected, and this energy is seldom picked as the onset of the *SVdiff* signal if there is a later impulsive onset. If the weak motion is picked, the magnitude of inferred shear wave splitting is reduced significantly. No isotropic or anisotropic structure has yet been shown to account for this reversed *SV* onset (which is intermittently observed beneath Alaska as well), and it may be a manifestation of scattering or heterogeneous general anisotropy.

Kendall and Silver [1996] assumed that the anisotropic region extends over the full 250 km thickness of D" beneath the Caribbean, and inferred 0.5-2.8% anisotropy over regions of 1000-2800 km in length. This can be compared with the estimate by *Doornbos et al.* [1986] that the *ScS* splitting of up to 2 s observed by *Mitchell and Helmberger* [1973] requires 2% anisotropy over a 75 km thick layer. The observed shift of the onset of *S* at 90° requires that the anisotropy is present at least several hundred kilometers above the CMB, not concentrated at the bottom of the thermal boundary layer as in the models of *Cormier* [1986]. In fact, for *S* waves that graze a shear velocity discontinuity, it is possible to account for the anisotropic effects by localizing anisotropic structure near the discontinuity rather than throughout the D" layer [*Garnero and Lay*, 1997; *Lay et al.*, 1997]. Absence of *SKS* splitting apart from that explained by receiver structure indicates that transverse isotropy is more likely than azimuthal anisotropy in this region.

Alaska. The region under Alaska and the northern Pacific has recently been studied by *Matzel et al.* [1996] and *Garnero and Lay* [1997]. *Matzel et al.* [1996] considered essentially the same WWSSN data as *Lay and Young* [1991], emphasizing the *S* observations in the distance range around 95°. Beyond 93° the apparent *SV* arrival onset is late relative to *SH* by 3 to 5 s (in 21 of 35 cases), as noted by *Lay and Young* [1991], and the *SH* waveforms show evidence of multiple arrivals associated with a shear velocity discontinuity near 243 km above the CMB, while the *SV* waveforms are simpler. Various isotropic models were explored but could not replicate these features. Given that the *SH* complexity is generated near the depth of the discontinuity, this suggests that anisotropy is present near that depth, as under the Caribbean. The primary contribution of this study was the computation of transverse isotropy synthetic seismograms using a reflectivity technique, with good agreement being achieved in the basic waveform behavior of the *SH* and *SV* signals near 95°. In a successful model (Figure 4b), the Vsh velocity structure has a 3% shear velocity discontinuity at a depth of 2600 km, with no

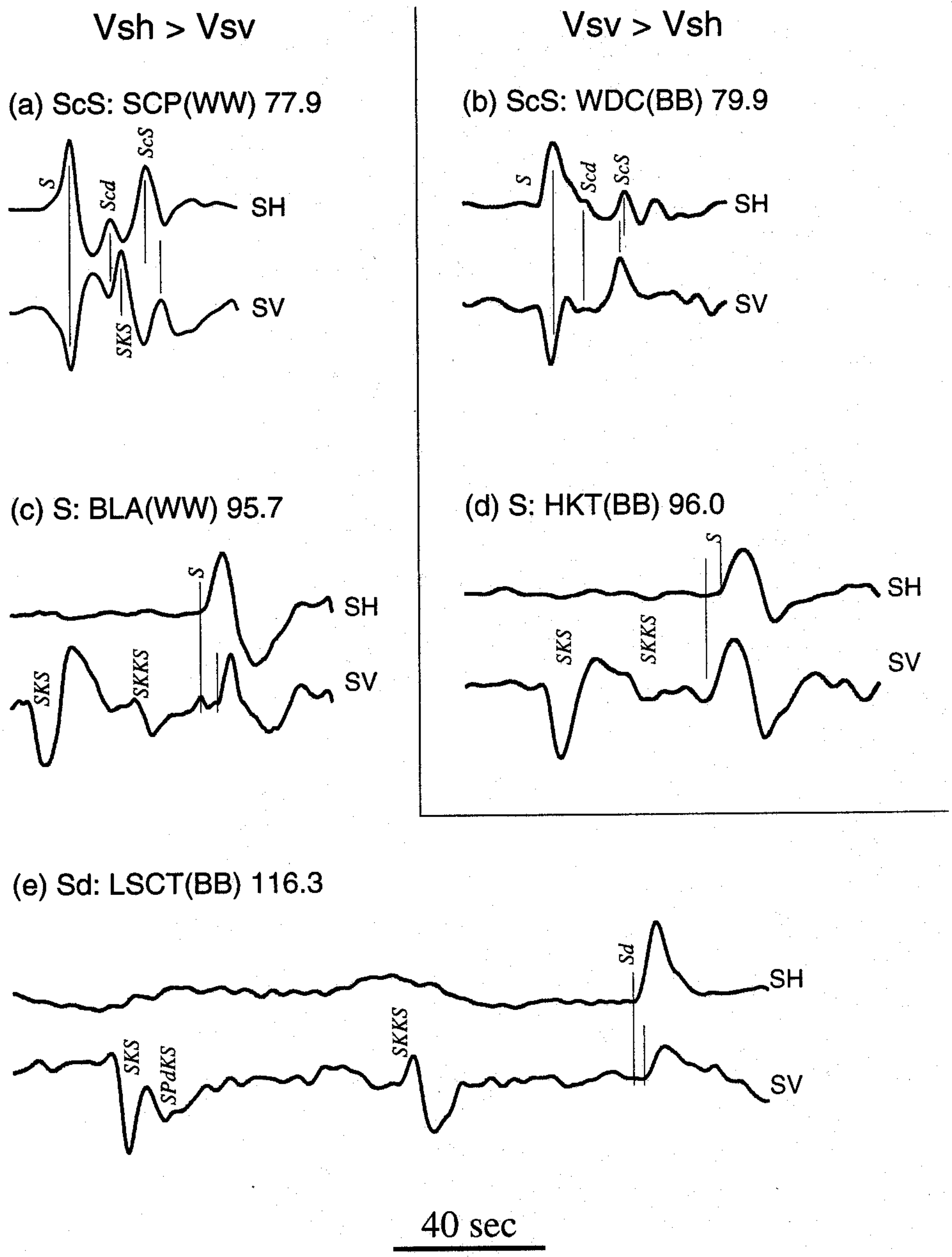

Figure 3. Representative shear waveform examples showing splitting between *SH* and *SV* components for each of the three phase geometries in Figure 2. (a) and (b) show relative shifts of *ScSH* and *ScSV* for paths under Alaska (a) and under the Pacific (b). The seismogram in (a) is the most extreme case for Alaska, with the first peak of *ScSH* (indicated by the vertical stroke) arriving more than 4 s ahead of the first peak of *ScSV*. The seismogram in (b) (kindly provided by Sara Russell), for the Pacific, shows the opposite behavior, but this appears to be fairly rare. (c) and (d) show examples of *S* waves near 95°, where the onset of the *SH* pulse is either earlier than *SV* (c), as under Alaska and the Caribbean, or later than *SV* (d), as intermittently observed under the Pacific (seismogram (d) was kindly provided by Jay Pulliam). (e) shows a long distance *Sdiff* observation traversing under the Pacific with Shdiff arriving ahead of *SVdiff*.

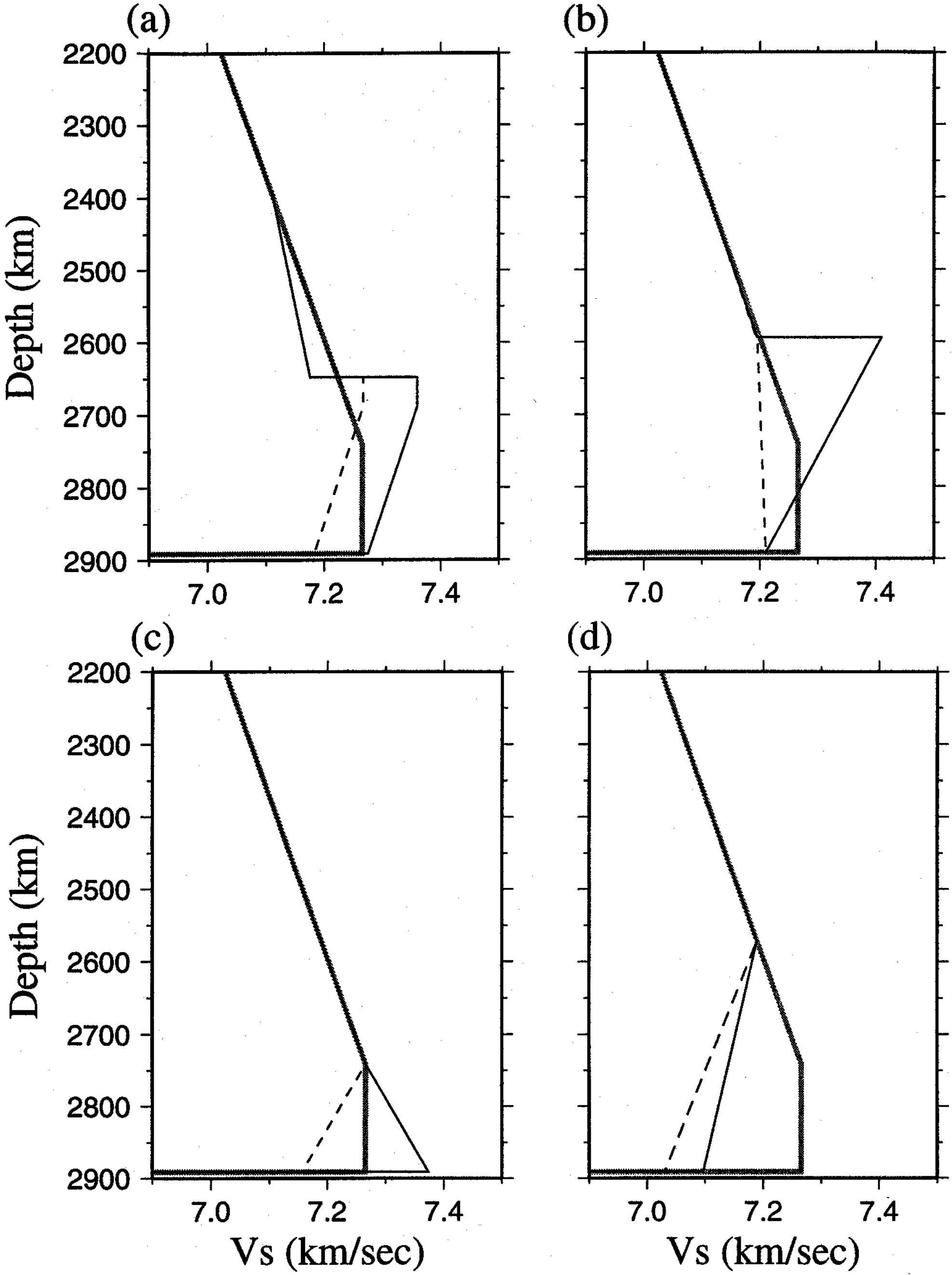

Figure 4. Classes of transverse anisotropy D" shear velocity models that have been proposed In various studies. The solid line indicates Vsh, the dotted line indicates Vsv, and the gray line indicates the shear velocity structure in PREM [*Dziewonski and Anderson*, 1981], which is the reference mantle model in each case. (a) is from study of the mantle under Alaska by *Garnero and Lay* [1997], and has a uniform anisotropy throughout the D" layer, along with a small Vsv discontinuity at the same depth as the strong Vsh discontinuity. (b) is from a study of the mantle under Alaska by *Matzel et al.* [1996], and reduces anisotropy within the D" layer. (c) is from *Maupin* [1994], and shows a class of models that was explored to model data under the Pacific observed by *Vinnik et al.* [1989], although not all signals could be matched with the same model. Anisotropy is concentrated in D". (d) is one of the models from *Vinnik et al.* [1995] which was used to model stacked waveforms from a cluster of Fiji events, with paths under the Pacific.

discontinuity in the Vsv structure. Anisotropy of 1.5-3% is needed to match the 3-5 s time lags. The D" discontinuity in this region thus appears to be stronger for Vsh than for Vsv, and there is evidence for either a small Vp discontinuity in this region [*Vidale and Benz*, 1993] or smooth radial structure [*Young and Lay*, 1989]. This led *Matzel et al.* [1996] to propose that the D" discontinuity is itself entirely an anisotropic transition in this region, primarily manifested in the Vsh structure.

Garnero and Lay [1997] further examine WWSSN and digital data traversing D" beneath Alaska, extending the mapping of laterally varying transverse isotropy initiated by *Lay and Young* [1991]. The resulting image obtained from a combination of path-length weighted *ScS* observations and *S* observations near 95°, is shown in Figure 5, with spatial smoothing applied to simulate the Fresnel zone effects of the long-period data. The anisotropy magnitude varies from 1.5% to zero over lateral scale lengths of 1000 km. Transverse isotropy models that successfully predict the waveforms of many (but not all) of the split signals are shown in Figure 4a, with a small, but non-zero shear velocity discontinuity in the Vsv structure being preferred due to observation of *SV* waveform complexities consistent with triplication by a small velocity increase [*Lay and Young*, 1991]. The anisotropy must exist near the discontinuity, but its variation with depth into D" is not constrained.

Garnero and Lay [1998] explore the effects of transverse isotropy in D" under Alaska on *SKS-SH* differential times. Anomalies of several seconds relative to reference structures are easily generated. It is notable that isotropic modeling of the *SKS-S* and *SKKS-SKS* differential time anomalies of several seconds for this region leads to incorporation of a low velocity layer in the outermost core to slightly delay the *SKS* or *SKKS* waves [*Lay and Young*, 1990], while including transverse isotropy in D" provides a more self-consistent explanation [*Garnero and Lay*, 1998].

Central Pacific. Recent studies of D" structure under the central Pacific have revealed substantial complexity, with a mix of observations of relatively slow *SV* (consistent with transverse isotropy), relatively fast *SV* (consistent with azimuthal anisotropy), and little or no shear wave splitting. This region is underlain by slower-than-average large scale shear velocity in most global tomography models [e.g. *Su et al.*, 1994; *Li and Romanowicz*, 1996], and anomalously large amplitudes of *SVdiff* observations traversing the lower mantle there indicate negative shear velocity gradients over the lowermost 200-300 km of the mantle [*Ritsema et al.*, 1997; *Valenzuela and Wysession*, 1998]. There is some evidence for a localized shear velocity discontinuity 175-185 km above the CMB [*Garnero et al.*, 1993; *Valenzuela and Wysession*, 1998], but it is likely that no discontinuity is present in much of the region. There is little evidence for a *P* velocity discontinuity in D" in this region [e.g. *Young and Lay*, 1989; *Wysession et al.*, 1998], while a thin very low velocity layer exists at the base of the mantle in extensive regions [see *Garnero et al.*, 1998]. These attributes differ from the circum-Pacific regions described previously.

Maupin [1994] presented a thorough, and sobering, theoretical study of effects of anisotropy in D", motivated by the observations of *Vinnik et al.* [1989]. She showed that the mere presence of *SVdiff* with amplitudes 30% of *SHdiff*, or isolated observations of complex *Sdiff* polarization with poorly defined onset times, does not uniquely resolve whether isotropic structure, transverse isotropy or azimuthal anisotropy is responsible. Using multiple events one can reliably detect azimuthal anisotropy if the horizontal particle motion of *Sdiff* proves independent of focal mechanism polarization (as noted above, there are some instances where the SV polarity near 95° is the same as that of SKS, which is inconsistent with the focal mechanism). Maupin favored the interpretation of azimuthal anisotropy for the *Sdiff* observations near 118°, but such a model could not fully explain all of the 3 higher quality observations of *Vinnik et al.* [1989], nor could models of transverse isotropy. In considering a suite of transverse isotropy models with different Vsv and Vsh gradients in D" (anisotropy was taken to increase with depth down to the CMB over a 150 km thick layer (Figure 4c)), Maupin found that shifts in the onset and first peak by 2.5 to 6 s can be achieved, as necessary to account for the observations near 95° in other regions by *Lay and Young* [1989] and *Kendall and Silver* [1996]. However, observed waveforms under the Pacific exhibit greater variability than predictions for any laterally uniform model, suggesting the importance of heterogeneous structure.

Vinnik et al. [1995] extended the *Sdiff* data set traversing the central Pacific, using recordings from 12 events at two east coast digital stations (HRV and WFM) at epicentral distances from 114° to 121°. The relative amplitude of motions identified as *SVdiff* to the usually clear *SHdiff* arrivals varied substantially, indicating little coupling between the two, and there was good correlation between *SVdiff* and *SKKS* amplitudes, indicating that source radiation pattern influences the *SVdiff* arrivals. This suggests that negative velocity gradients in D" are present, in order to have *SV* energy penetrate deep into the shadow zone. A 3 s shift of onset time of *SVdiff* relative to *SHdiff* was also measured for a stack of signals from 6 events from 116° to 120°, although one has to be concerned that the focal mechanisms and distances differ for the stacked traces.

Reflectivity synthetics [*Kind and Müller*, 1975] were used to separately model the *SH* and *SV* components under the hypothesis of transverse isotropy, and *Vinnik et al.* [1995] were able to explain three features of the stacked data: (1) anomalously late *SHdiff* arrivals (up to 10 s later than the reference IASP91 model), (2) the 3 s delay of the onset of *SVdiff* with respect to *SHdiff*, and (3) different spectral content of *SVdiff* and *SHdiff*, with *SVdiff* peaking

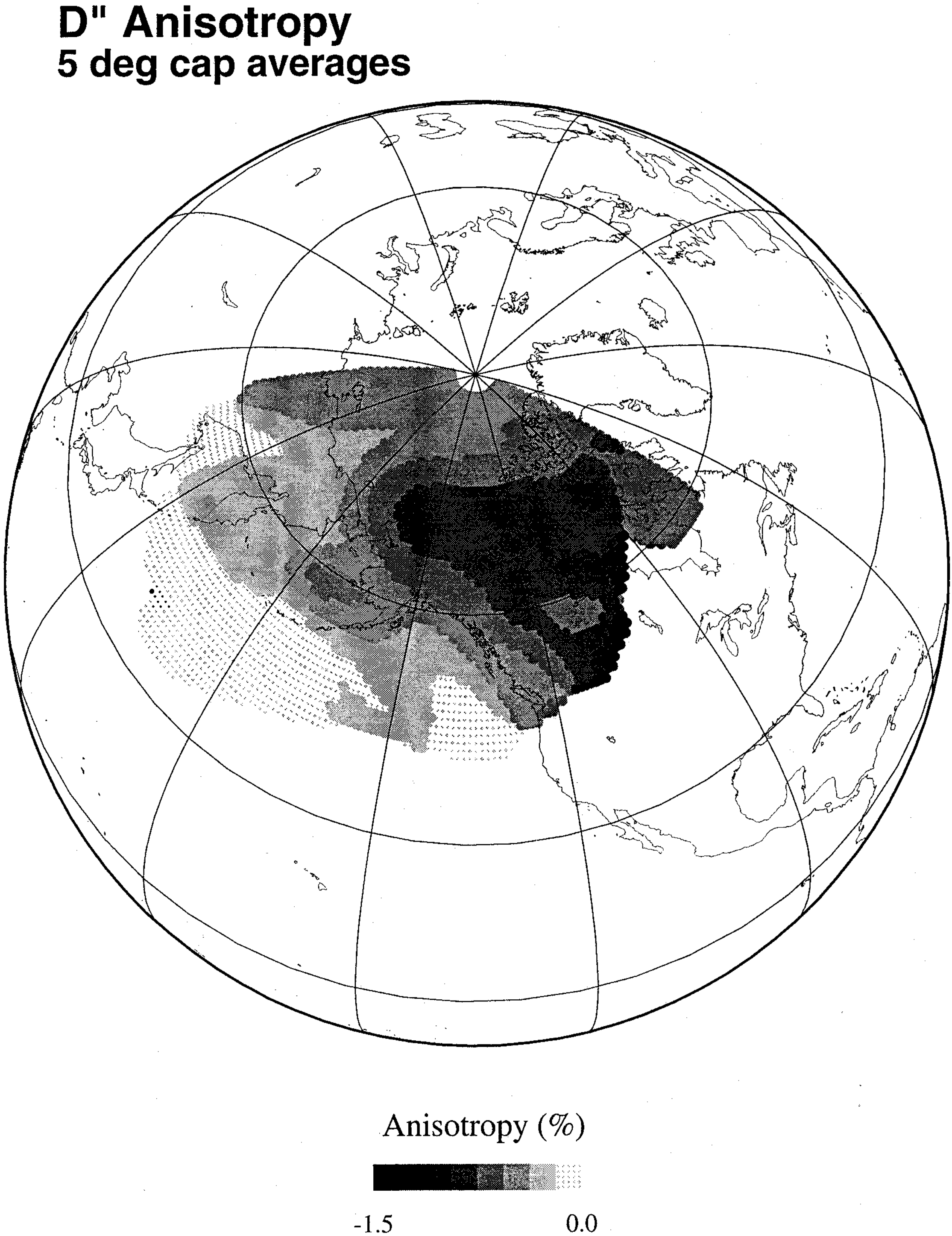

Figure 5. Map of lateral gradients in anisotropy in the lowermost mantle beneath Alaska, showing how the transverse isotropy appears to increase from west to east. [from *Garnero and Lay*, 1997].

at a higher frequency. The observations can be explained by a model with a low Vsh layer with a thickness of 250-350 km with Vsv even slower by about 1%. Alternative models featured negative gradients in the same depth range with equivalent velocity reductions, which are more compatible with profiles of *SVdiff* data modeled by *Ritsema et al.* [1997]. Figure 4d indicates successful anisotropic models with negative gradients that fit the *SVdiff/SHdiff* spectral ratios and the 3 s travel time shift [*Vinnik et al.*, 1995]. Four events from 114° to 115° showed no splitting, indicating that anisotropy is laterally varying in this region, and there is little constraint on the vertical distribution of anisotropy within the D" region (it need not be distributed over the entire depth range in which the shear velocity decreases). It appears that transverse isotropy may be present in lower mantle with either faster-than-average or slower-than-average velocities.

Garnero and Lay [1997] considered a profile of broadband recordings in North America from a Fiji event, with no apparent splitting at 95°, about 1 s delay of the onset of *SVdiff* relative to *SHdiff* at 102°, and 3.3 s relative delay of *SVdiff* at 116.3° (see Figure 3e). The latter number is consistent with the 3 s delay seen by *Vinnik et al.* [1995] at east coast stations. *Kendall and Silver* [1998] report negligible splitting at Canadian stations for paths under the central Pacific, with the exception of small amounts of splitting at distances larger than 110° (to Central and Eastern Canada), which is consistent with the profile of *Garnero and Lay* [1997]. However, observations in Northwestern Canada do show increasing delays of *SVdiff* onset with distance [*Ritsema et al.*, 1998]. It is possible that a lateral gradient of increasing transverse isotropy structure toward the North American continent is sensed by these data.

Pulliam and Sen [1998] considered a small data set at closer ranges, finding 3 records with *SV* advances of up to 2.2 s relative to *SH* at distances from 93.9° to 96° at a station in Texas (corrected for receiver anisotropy), one of which is shown in Figure 3d. Some stations at closer distances show no splitting for the same events, so it was inferred that the anisotropy is near the base of the mantle. An azimuthal anisotropy model with Vsv having a positive velocity increase in the lowermost 150 km of the mantle, while Vsh is nearly constant, gives good waveform matches to the data. The independent evidence for a regionally extensive negative gradient in the sub-Pacific Vsv structure casts some doubts on the specific model used, but the observation of intermittent early *SVdiff* arrivals is supported by other work [*Vinnik et al.*, 1998; *Ritsema et al.*, 1998].

Analysis of broadband *ScS* recordings in western North America (see Figure 3b) indicates small scale variations in anisotropy with the fast polarization sometimes being close to the longitudinal component and sometimes close to the transverse component [*Russell et al.*, 1998]. The data vary systematically over scale lengths of only a few hundred kilometers, indicating that is unwise to make generalizations about anisotropic structure from sparse data distributions.

While a better azimuthal distribution of seismic data will be required before azimuthal anisotropy in the lowermost mantle can be constrained, certain *ScS* and *SHdiff* profiles are compatible with this possibility. *Winchester and Creager* [1997] infer azimuthal anisotropy from azimuthal patterns in transverse *ScS-S* travel time differentials for three different D" locations beneath the western Pacific. This interpretation assumes that *ScS* is the anomalous phase, and that the anomalies arise from the same lower mantle volume. *Valenzuela and Wysession* [1998] find azimuthal variation in *SHdiff* profiles in D" beneath northeastern Siberia. Most profiles trending SE-NW are 1-3% faster than for PREM [*Dziewonski and Anderson*, 1981], while most profiles trending SW-NE are 1-2% slower than for PREM. Given the differences in path in a heterogeneous region, the interpretation in terms of azimuthal anisotropy is very tentative.

Vinnik et al. [1998] consider profiles of observations at individual stations in North America in the range 92° to 122° from Fiji events to explore anisotropic structure under the Pacific. Station profiles of differential travel time residuals for *SKS-S* and *SKKS-S* show increases with distance indicative of accumulating delay of *S* in a low velocity layer at the base of the mantle. Changes in the rate of increase with distance are attributed to strong lateral gradients of Vsh in a layer about 300 km thick, with velocities as much as 10% lower than PREM. In the southwestern region of the model, Vsh returns to "normal" over a distance of only several hundred km, while Vsv remains low by about 10%, suggesting very large anisotropy. Several stations display small increases in *SVdiff-SHdiff* differential arrival times with increasing distance, supporting some increase in isotropy toward the southwest. The strength of the lateral gradients and magnitude of the anisotropy are highly dependent on interpretation of the distance trends, particularly the assumption of a 300 km thick zone of anomalous structure. The very low Vsv in the southwestern area is compatible with observed *SKKS-SKS* travel time residuals of 2-3 s that likely originate in the same region [*Schweitzer and Müller*, 1986; *Garnero and Helmberger*, 1993]. In the central region where Vsh is very low, a few observations of early *SVdiff* are reported, consistent with *Pulliam and Sen* [1998] and *Russell et al.* [1998].

Clearly, more work is needed, but a preliminary synthesis of observations under the Pacific is that there are strong lateral gradients in isotropic and anisotropic structure in the low velocity central region, fringed by regions to the northeast and southwest that may have transverse isotropy (see Figure 1). The spatial gradients are poorly resolved, as are the overall extent and magnitude of anisotropy.

GEODYNAMICAL AND MINERAL PHYSICS CONSIDERATIONS OF D" ANISOTROPY

The underlying physical origin of anisotropy in D" must be addressed by considering a suite of scenarios involving physical properties under conditions not yet extensively explored in the laboratory. At the most basic level, that D" anisotropy is detectable in the regions shown in Figure 1 and (apparently) not observed in the bulk of the lower mantle indicates that fundamental differences in length scales, structure, deformation style and/or chemistry exist between the lowermost mantle and the overlying material. As noted by *Karato* [1989], identifying the dominant deformation mechanisms (dislocation motions, grain boundary diffusion, melt alignment) and controlling factors (strain versus stress) that can give rise to anisotropy requires knowledge of the flow regime or vice versa. Current ignorance of the detailed chemistry, physical properties and flow regime in D" limits our ability to interpret anisotropy in the region.

It is probable that a hot, low viscosity thermal boundary layer (TBL) is present at the base of the mantle [e.g., *Loper and Lay*, 1995]. Conventional estimates of the TBL thickness suggest 50-75 km [e.g., *Stacey and Loper*, 1983], however, the evidence described above for much thicker zones of negative velocity gradient in D" beneath the central Pacific, Alaska, and the Caribbean suggests that the TBL may actually be 200-250 km thick. The TBL dynamic regime is embedded the within larger scale circulation of the lower mantle induced by downwellings (maybe involving slabs), internal heating, and upwellings in "superplumes" or plume provinces. Strong horizontal shear flows are likely in the low viscosity TBL, and thermal instabilities may give rise to small-scale upwellings [e.g., *Olson et al.*, 1987]. Upwelling plumes will tend to entrain material up to a few percent denser than the overlying mantle [e.g., *Davies and Gurnis*, 1986; *Sleep*, 1988; *Hansen and Yuen*, 1988; *Olson and Kincaid*, 1991]. In numerical simulations, the entrained material tends to form vertically oriented "cusps".

Another distinct attribute of the lowermost mantle is the proximity of the huge density contrast at the CMB. Given the long history of chemical differentiation of the planet, D" is a likely depository for chemical heterogeneities with densities intermediate to those of the lower mantle and core. D" chemical heterogeneities may arise from many processes, including chemical reactions between the core and mantle, chemical distinctions associated with relic slabs, and chemical fractionation associated with partial melting at the base of the mantle. The chemical buoyancy and physical characteristics of any chemical heterogeneity will determine how it interacts with the TBL flow regime.

The probable thermal and chemical complexity of D", coupled with the lack of experimental constraints on lower mantle deformation processes at relevant pressure and temperature conditions, has generated an abundance of possible causes for the anisotropy in D" (Figure 6) [*Wysession*, 1996; *Karato*, 1997]. Two major families of mechanisms are those involving large-scale structural anisotropy and those involving lattice preferred orientation (LPO) of minerals within this region. The former family postulates a broad range of possible heterogeneities in chemistry or phase incorporated within D"; the latter family most likely involves either a change in chemistry, phase, or deformation style from the overlying mantle. Accordingly, the basic observation of anisotropy within D" reemphasizes the anomalous character of this zone relative to the overlying mantle.

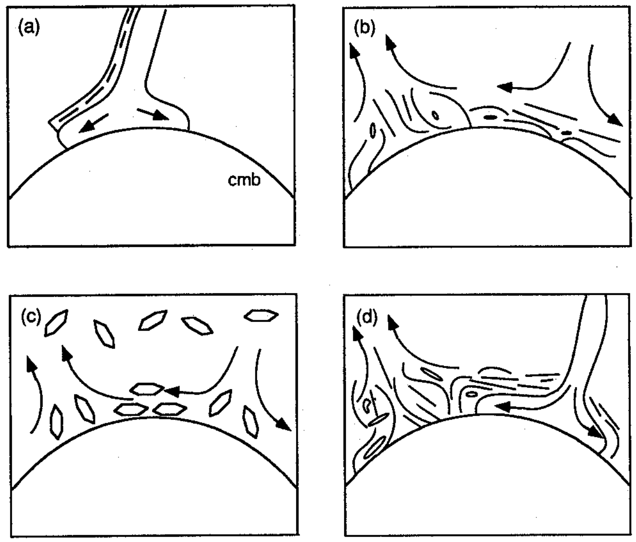

Figure 6. Schematic illustrations of possible dynamically induced anisotropic structure in D". (a) Subducted slabs, retaining anisotropic fabrics, or having melting/deformation of crustal components accumulate in D" and produce transverse isotropy associated with the D" discontinuity in faster-than-average areas. (b) Core-mantle chemical reaction products and/or partial melt components from the thermal boundary layer are entrained in large-scale boundary layer flow and sheared to make lamellae with strong velocity contrasts. This can produce both general and transverse isotropy concentrated near the CMB. (c) Lattice preferred orientation (LPO) in primary lower mantle minerals is organized by strong boundary layer shear flows. A transition in deformational mechanism, perhaps under the high temperatures of the boundary layer is responsible for the enhanced anisotropic fabric developed in the D" region. (d) Chemical heterogeneities and/or partial melt components are sheared into vertical lamellae near the CMB beneath upwellings and ride up over the top of downwelling slab structures to produce transverse isotropy near the D" discontinuity.

Structural Anisotropy in D"

Proposals of structurally-induced anisotropy in D" have emphasized mechanisms that give rise to finely laminated structures with strong contrasts in material properties.

Horizontally laminated structures will yield *SH* velocities faster than *SV* [*Backus*, 1962; *Kendall and Silver*, 1996], in general accord with most shear wave splitting in D". Mechanisms which could generate such laminated structures within a TBL at the base of the mantle include entrainment of core-mantle reaction products in the lowermost mantle [*Knittle and Jeanloz*, 1991]; injection of subducted oceanic crustal material into the boundary layer, perhaps associated with partial melt [*Kendall and Silver*, 1996]; and diking induced by either the presence of partial melt or of solidified partial melt near the CMB [e.g. *Williams and Garnero*, 1996]. Even small pockets of partial melt will tend to be sheared by flow, creating a fabric with shaped preferred orientation (SPO), but the chemical buoyancy and distribution of the melt will play an important role in whether such a fabric is sustained or whether the melt drains out (either upward or downward). In short, such laminations could be: generated by interactions with the core below; derived from geochemical heterogeneities produced from tectonic processes; a manifestation of the presence of melt in this region; or some combination of these.

Core-mantle chemical reactions have been demonstrated as viable at the CMB based on both experimental data [*Knittle and Jeanloz*, 1989; 1991; *Goarant et al.*, 1992] and thermochemical calculations [*Song and Ahrens*, 1994]. Notably, CMB reactions appear to be significantly enhanced by the presence of partial melt [*Ito et al.*, 1995; *Williams*, 1998]. The distribution of reaction products within laminar structures is inferred from their being generated at the CMB, with subsequent entrainment into the overlying mantle. Two types of laminations can plausibly arise. First, unreacted mantle could be juxtaposed with lamellae containing a mixture of the reaction products: this possibility has been examined by *Kendall and Silver* [1996] who noted that iron-enrichment and reaction within D" could produce the observed anisotropy of D", but would likely lower the shear velocity of the iron-enriched zone by up to 6%. Second, any physical separation between the relatively high seismic velocity (and lower density) iron-free perovskite and silica reaction products and the iron alloy reaction products would give rise to three possible combinations of materials which could produce laminar features: seismically fast iron-depleted reaction products, markedly slow (by approximately 40% in shear [*Kendall and Silver*, 1996; *Williams and Garnero*, 1996]) iron alloys, and unreacted mantle. *Pulliam and Sen* [1998] suggest that azimuthal anisotropy beneath the central Pacific is caused by entrainment of chemical heterogeneities, perhaps from CMB chemical reactions, in upwelling flows, or possibly in a shear zone between flows with opposing directions. A horizontal symmetry axis for the resulting lateral 'lamination' can account for the shear wave splitting. Although the precise mechanisms of, and scale-lengths at which, such reaction-induced geochemical heterogeneities are entrained into the overlying D" layer remain conjectural, the recognition that D" may be associated with low viscosity, partially molten and plausibly rapidly flowing material provides a number of possible entrainment and emplacement mechanisms for such reaction products.

If lithospheric slabs sink to the D" region (Figure 6a) [e.g. *Christensen and Hofmann*, 1994; *Grand et al.*, 1997] their influence on anisotropy in D" depends greatly on their thermal, mechanical and chemical structure. Numerical simulations [e.g., *Tackley*, 1995] indicate that slabs could accumulate in the transition zone before descending into the lower mantle in large blobs, sustaining strong thermal anomalies all the way to the CMB. Thus, slabs could enhance lateral temperature variations in D". Slabs may also undergo significant internal deformation as they descend; the eclogitic component may delaminate from the residual slab. The separate components may break up and stretch to form lamellae whose orientation would depend not only the local flow regime, but on the integrated flow history [e.g., *Gurnis*, 1986]. Subducted slabs approaching the CMB will tend to form laterally-aligned tendrils as the slab folds and spreads out along the base of the mantle, possibly disrupting any compositionally distinct layer and perhaps contributing slab derived heterogeneities as well (Figure 6d).

The chemical properties of slabs also influence whether anisotropy results. The basaltic chemistry material is likely to be juxtaposed with mantle of approximately peridotitic chemistry and, if the slab retains its initial stratification, a harzburgitic (olivine-enriched) layer near its former base (Figure 6a). The degree to which purely solid-state elastic differences between basalt and either peridotitic or harzburgitic chemistry can generate differences in shear velocity is unclear. The basaltic layer is anticipated to be enriched in $CaSiO_3$-perovskite and to have an enhanced iron and aluminum content present within $(Mg,Fe)SiO_3$-perovskite relative to the surrounding material; the formerly basaltic material may also contain small (~10%) amounts of free SiO_2 [*Irifune and Ringwood*, 1987; *Irifune*, 1994; *Kesson et al.*, 1994]. Unfortunately, the elastic properties of Al- and Fe-enriched magnesium silicate perovskite are ill-constrained, as is the shear modulus of calcium silicate perovskite (and, of equivalent importance for the conditions of the CMB, the pressure derivative of the shear modulus of both calcium and magnesium silicate perovskites). As a result, it is difficult to assess the magnitude of solid-state shear velocity contrasts between layers of basaltic chemistry, their complementary harzburgitic layers, and peridotitic mantle under CMB conditions.

Kendall and Silver [1996] propose that D" anisotropy may be associated with the presence of melt inclusions within the basaltic layer: such melting could be associated with a depression of the eutectic temperature associated with enhanced Ca, Al and Fe contents or, speculatively, even with the retention of volatiles within the subducted oceanic crust to ultra-high pressures. Aligned inclusions of melt can readily produce *S* wave anisotropy, with the magnitude of anisotropy at a given melt fraction hinging crucially on the aspect ratios of the inclusions [*Kendall and*

Silver, 1996]. For small aspect ratio inclusions (0.01), as little as 0.5% partial melting could give rise to the observed anisotropy. *Karato* [1997] argues that melting of slab components seems unlikely because the downwelling regions are likely to be the coldest portions of D". Perhaps a stronger argument is that it is unclear what flow regime in the downwelling could produce the multiple oscillating, or anastamozing layers of material with few kilometer scale lengths required to produce a seismically anisotropic fabric (a single, or even a few layers will not suffice).

Partial melt in D" need not involve slabs; *Williams and Garnero* [1996] interpret the ULVZ in terms laterally varying partial melt concentrations of between 5 and 30% in the lowermost 5-40 km of the mantle. Such large-scale melting in the lowermost mantle could easily give rise to very large values of *S* wave anisotropy if the orientation of the melted material is only marginally aligned in a horizontal direction. Although the distribution of partial melt as a function of depth within D" is not clear, the existence of large-scale melting in the lowermost regions of D" raises the crucial issue of the depth dependence of anisotropy within this zone. That is, depending on the degree of preferred alignment of melt in the lowermost mantle, even a modest sampling of the lowermost mantle could result in the observation of *S* wave anisotropy. In short, if liquid is present in abundance within the lowermost mantle, and this region experiences significant strain, preferred alignment of melt inclusions would be expected.

As an additional effect, depending upon the detailed geographic distribution and thickness of the partially molten ULVZ over time and the overall stability of the D" region with respect to deformation and entrainment in the overlying flow of the lower mantle [e.g., *Sleep*, 1988; *Kellogg and King*, 1993], regions which contained a ULVZ in the past may retain a structural anisotropy produced by the presence of laminations of solidified partial melt. In particular, the thickness of the ULVZ through geologic time remains obscure: if, as is likely, the mantle has undergone secular cooling, a thicker and more widespread ULVZ would be expected to have been present in the past. The level at which fossil remnants of a more pervasive partially molten zone are preserved depends on both their detailed chemistry (which controls the buoyancy of such features) and the dynamics of the lowermost mantle: simulations suggest that an augmentation of only a few percent in density is needed to stably stratify the lowermost mantle for extended periods of geologic time [*Sleep*, 1988]. While speculative, the role of solidified dike- or laccolith-like features in generating anisotropy in D" hinges critically on how different the composition of melt generated near the CMB is from the composition of normal mantle. That is, the degree to which the eutectic composition in the CMB differs from the bulk composition of the lower mantle represents a crucial parameter in determining whether such fossilized melt regions could have markedly different shear wave velocities from normal mantle.

These disparate mechanisms of producing structural laminations; swept-up CMB reaction products, emplacement of subducted oceanic crust, and preferred orientation of partially molten material (or its fossilized remnants) at the CMB, can each fulfill the fundamental requirement of producing an intercalation of material of differing shear modulus within the material of the lowermost mantle. Yet, each mechanism does have specific implications, requirements and first-order uncertainties associated with it. It is also important to note that these mechanisms need not operate to the exclusion of one another.

Intrinsic Mineralogical Anisotropy in D"

Any LPO that develops in D" will depend on the strain experienced by grains, the grain size, and the dominant deformation mechanism(s) active there. *Kellogg and Turcotte* [1990] showed that the amount of strain on a marker in mantle flow is largely controlled by the time it spends undergoing pure shear. Thus, LPO is likely to be greatest in the vicinity of strong horizontal flows and near active upwellings and downwellings, where the strain rates are highest (Figure 6c). Strain patterns within D" may not correspond directly to flow in the overlying mantle, as small scale circulation within D" can decouple the strain patterns from the overlying upwellings and downwellings, so it is very difficult to infer any particular strain regime in D". Given that the entire mantle is straining, it is important to account for LPO being concentrated at the base of the mantle.

The primary means by which anisotropy could be generated by LPO in D", but not in the overlying mantle (without invoking a change in chemistry) are through a dramatic difference in the strain history of the lowermost mantle from the overlying material, a phase change of one of the constituents of the lowermost mantle, and/or a shift in deformational mechanism within (or just above) D". The viability of the first of these mechanisms is difficult to assess, given the profound uncertainties in the flow field of the lowermost (or for that matter, lower) mantle. The second of these mechanisms, the presence of a phase change in the lowermost mantle which could in turn give rise to LPO within a new assemblage is extremely speculative: although possible phase changes in deep mantle constituents have been sporadically reported based on both theoretical and experimental grounds [*Cohen et al.*, 1997; *Cohen*, 1992; *Meade et al.*, 1995a; *Saxena et al.*, 1996; *Stixrude et al.*, 1996], each of these proposed transitions suffer from one of the following difficulties: 1) they are not necessarily coincident with the pressures at the top of D", but rather may occur in the mid-mantle [*Meade et al.*, 1995a; *Saxena et al.*, 1996; *Stixrude et al.*, 1996]; 2) they are not observed in shock experiments on compositions expected to be similar to those in the lowermost mantle [*Cohen et al.*, 1997; *Vassiliou and Ahrens*, 1982]; or 3) they hinge on the presence of abundant SiO_2 in the deep mantle [*Cohen*, 1992], a mineralogy which is unlikely to occur in an isochemical mantle unless perovskite is destabilized at high pressures: a possibility that is highly controversial [e.g., *Knittle and Jeanloz*, 1987; *Kesson et al.*, 1994]. A chemically distinct D" layer could enable phase transitions to occur that would not be expected within a homogeneous lower mantle, but this possibility is almost unconstrained. At present, we consider a shift in deformational mechanism to be the most viable for generating LPO in D", given the low pressure rheologic behavior of materials, speculations on the rheologic behavior of the lower mantle, and the role of D" as a TBL.

In particular, the lack of anisotropy in the lower mantle has been attributed to the deformational mechanism of perovskite not giving rise to preferred orientation based on ambient temperature, high-pressure experiments on perovskite deformation [*Meade et al.*, 1995b]. The observed average shear wave elastic anisotropy of perovskite is in excess of 6% [*Meade et al.*, 1995b; *Yeganeh-Haeri*, 1994], with a peak shear velocity anisotropy of 16% [*Yeganeh-Haeri*, 1994]; other possible lower mantle phases (MgO, SiO_2) have similar magnitudes of maximum anisotropy [*Meade et al.*, 1995b; *Jackson and Niesler*, 1982; *Weidner et al.*, 1982]. Notably, the degree to which these elastic anisotropies will change at the conditions of the CMB is unclear: studies of the pressure-dependence of anisotropy at ultra-high pressures remain in their infancy, but there are both theoretical and experimental indications that the level of anisotropy in lower mantle minerals could be quite different at high pressures [e.g., *Duffy et al.*, 1995; *Karki et al.*, 1997]. Based on ambient temperature results, *Meade et al.* [1995b] observed essentially no formation of anisotropic textures within sheared silicate perovskite, and proposed that the available slip systems of perovskite are such that they do not give rise to anisotropic textures under deformation. Whether this result remains robust at high temperatures remains unclear [e.g., *Karato et al.*, 1995].

For comparison, *Karato et al.* [1995] proposed, based on high temperature and low pressure (0.3 GPa) deformation results on an analogue material ($CaTiO_3$), that deformation of the lower mantle could occur within a superplastic regime, in which grain boundary sliding provides the dominant means of deformation. In general, such superplastic deformation does not produce anisotropic textures. In a number of materials (including olivine, ice and silicon), increasing temperature while holding shear stress constant can yield a rheologic transition from such plastic deformation into a power-law deformation regime [e.g., *Frost and Ashby*, 1982]. Such a transition would be expected to yield a transition from largely isotropic textures to anisotropic textures: as present estimates of the temperature jump across D" are typically in excess of 800 K [*Williams and Jeanloz*, 1990; *Boehler*, 1993; *Williams*, 1998], homologous temperature changes of the order of 0.3 are expected across D". Such large shifts in homologous temperature lie in a range which could readily drive the behavior of the lowermost mantle from predominantly plastic flow into a power-law creep regime. This change in deformation mechanism would be expected if (1) the boundary between the plastic and power-law flow regimes exists under conditions of the deep mantle, and has a positive slope in the shear-stress/homologous temperature plane; and 2) if the lower mantle does actually deform in a superplastic regime [e.g. *Karato et al.*, 1995]. As a result, a shift from plastic to power-law flow could plausibly alter the rheology of the lowermost mantle in a manner that could result in anisotropy being generated within D", but not within the overlying mantle. *Karato* [1997] favors such a possibility for D" anisotropy, with strong elongation of MgO minerals in a high viscosity perovskite matrix. The anisotropy of D" could be intimately associated with the temperature jump across this zone, and be a fundamental manifestation of a different deformational process occurring within D" relative to the overlying lower mantle.

DISCUSSION AND CONCLUSIONS

We do not yet have a full understanding of anisotropy in D", and many fundamental issues need to be resolved. However, it is clear that observations of anisotropy hold potential for constraining processes taking place at the base of the mantle. Distinguishing between various scenarios like those in Figure 6 will be challenging, as each has attendant uncertainties at the heart of the mechanism for generating anisotropy. One source of guidance is provided by relating the observations of anisotropy to large-scale patterns in mantle structure. This is considered in Figure 7, which compares observed anisotropic characteristics (Figure 7a) with the spatial distribution of ULVZ in D", a model of subducted slab that may have penetrated to D", and buoyancy-flux weighted hot spots (Figure 7b), and with spatial patterns in deep mantle shear velocity structure from a high resolution tomographic inversion (Figure 7c). There is a general spatial association of regions with transverse isotropy and areas of subducted slab accumulation and absence of a detectable ULVZ. Transverse isotropy tends to be observed in faster than average lower mantle, while the slow region of the central Pacific exhibits small-scale general anisotropy. Extending these spatial correlations is one important direction for future research.

The most plausible mechanisms for generating anisotropy near the base of the mantle appear to be either the development of sheared lamellae of partial melt or chemical heterogeneities or the development of LPO if there is a transition in predominant deformation mechanism in the hot boundary layer. Multiple mechanisms for generating anisotropy may be operative; for example, it is difficult to reconcile all observations with downwelling slab structures. However, the latter may play an important role if they displace chemical heterogeneities in D" as they sink to

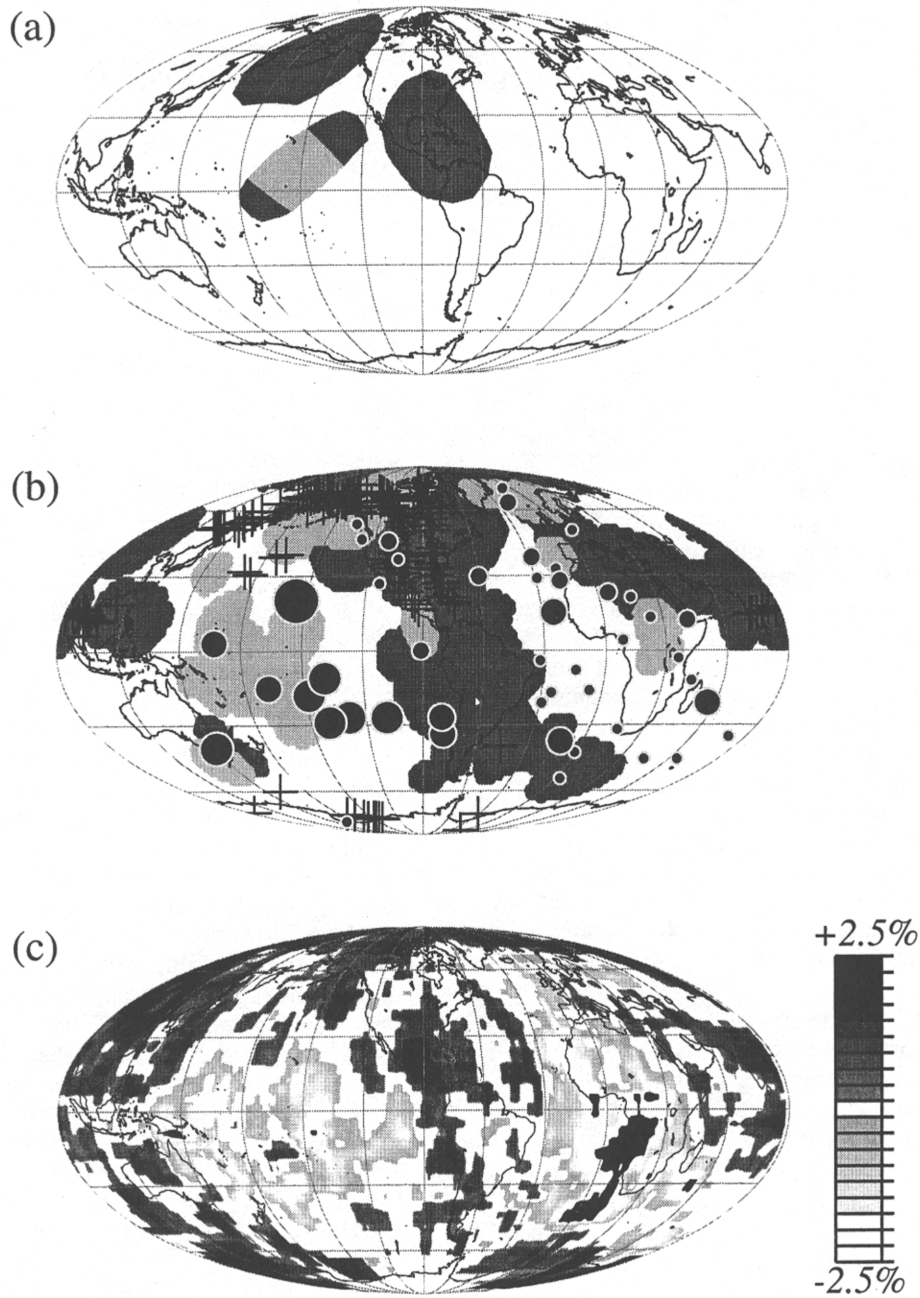

Figure 7. (a) Locations where shear wave has been observed in the D" region from Figure 1. Darker areas are consistent with transverse isotropy while the mid-Pacific lighter area has a mix of general and no anisotropy. (b) Locations where a thin very low velocity region at the base of the mantle (light shaded areas) has been observed or not (dark areas), along with hotspot locations indicated by circles with sizes proportional to estimated buoyancy flux (from *Garnero et al.* [1998]). Also shown are the regions of subducted slab that may have reached the base of the mantle (plus signs) from the model of *Lithgow-Bertelloni and Richards* [1997]. (c) Lateral variation in the shear velocity structure at a depth of 2750 m from the tomographic model reported in *Grand et al.* [1997].

the CMB, with the in situ material riding up horizontally on top of the ponding slab to produce anisotropic structure several hundred kilometers above the CMB [e.g. *Wysession*, 1996]. This could reconcile observations of anisotropy at the CMB in hot areas and well above it in colder areas.

Important research efforts need to be undertaken. Seismological work needs to expand the spatial sampling of D", to establish any systematic relationships between D" anisotropy and large scale structure in D" and the overlying mantle, and to investigate localized regions to establish the variability of anisotropy on small scale lengths. These efforts should include attempts to detect *P* velocity anisotropy, particularly in areas like the mid-Pacific where general anisotropy is suggested by the *S* wave splitting results. Continued characterization of shallow mantle and near source contributions to anisotropic measurements must be sustained as well. Geodynamical topics include boundary layer calculations for materials with strong viscosity contrasts, such as in the case of partial melt, to assess fabric development in the presence of shear flow. With the evidence for a thick thermal boundary layer (200-300 km thick) in the Central Pacific, along with regions of partial melt underlying this zone, dynamical models used to assess entrainment and boundary layer instability need to be reconsidered. Experimental constraints on deformation mechanisms operating under D" pressure and temperature conditions are essential for assessing whether LPO in perovskite and magnesiowustite can actually develop in strong shear flows in a hot boundary layer. It is also important to assess the physical properties of possible partial melt components in D", along with those of slab remnants to assess whether SPO of sufficient strength to explain the seismic data can actually develop or not. The stability of orthorhombic perovskite and the possibility of enhanced stishovite content in the D" layer must be further explored. All of these topics are at the leading edge of research in each discipline, but it appears that by understanding anisotropy in D" we will significantly advance our understanding of deep Earth processes.

Acknowledgments. GMT mapping software of *Wessel and Smith* [1991] was used in figures. C. Lithgow-Bertelloni and S. Grand provided slab and seismic tomography models, respectively. We thank J. Pulliam for providing some of his waveform data in advance of publication. B. Romanowicz, J. Ritsema, D. Helmberger and an anonymous reviewer provided comments on the manuscript. This research was supported by NSF grants EAR 9305894, EAR 9418643 (T.L.) and 9896047 (E.J.G.). Workshops on the core-mantle boundary organized under EAR 9305894 helped develop interdisciplinary coordination. Contribution 337 of the Institute of Tectonics and the W. M. Keck Seismological Laboratory.

REFERENCES

Anderson, D. L., Thermally induced phase changes, lateral heterogeneity of the mantle, continental roots, and deep slab anomalies, *J. Geophys. Res., 92*, 13968-13980, 1987.

Backus, G. E., Long-wave elastic anisotropy produced by horizontal layering, *J. Geophys. Res., 67*, 4427-4440, 1962.

Boehler, R., Temperatures in the Earth's core from melting-point measurements of iron at high static pressures, *Nature, 363*, 534-536, 1993.

Christensen, U. R., and A. W. Hofmann, Segregation of subducted oceanic crust in the convecting mantle, *J. Geophys. Res., 99*, 19867-19884, 1994.

Cohen, R. E., First principles predictions of elasticity and phase transitions in high pressure SiO_2 and geophysical implications, in *High Pressure Research: Application to Earth and Planetary Sciences*, Eds. Y. Syono and M. H. Manghnani, pp. 425-431, American Geophysical Union, Washington, D.C., 1992.

Cohen, R. E., I. I. Mazin, and D. G. Isaak, Magnetic collapse in transition metal ions at high pressure: Implications for the Earth, *Science, 275*, 654-657, 1997.

Cormier, V. F., Synthesis of body waves in transversely isotropic Earth models, *Bull. Seism. Soc. Am., 76*, 231-240, 1986.

Cormier, V. F., Anisotropically distributed heterogeneity in D", *EOS Trans. AGU, Fall Meeting Suppl., 76 (46)*, F402, 1995.

Davies, G. F., and M. Gurnis, Interaction of mantle dregs with convection: Lateral heterogeneity at the core-mantle boundary, *Geophys. Res. Lett., 13*, 1517-1520, 1986.

Ding, X., and D. V. Helmberger, Modeling D" structure beneath Central America with broadband seismic data, *Phys. Earth Planet. Int., 101*, 245-270, 1997.

Doornbos, D. J., and J. C. Mondt, *P* and *S* waves diffracted around the core and the velocity structure at the base of the mantle, *Geophys. J. Roy. Astron. Soc., 57*, 381-395, 1979.

Doornbos, D. J., S. Spiliopoulos and F. D. Stacey, Seismological properties of D" and the structure of a thermal boundary layer, *Phys. Earth Planet. Inter., 41*, 225-239, 1986.

Duffy, T. S., R. J. Hemley, and H. K. Mao, Equation of state and shear strength at multimegabar pressures: Magnesium oxide to 227 Gpa, *Phys. Rev. Lett., 74*, 1371-1374, 1995.

Dziewonski, A. M., and D. L. Anderson, Preliminary reference Earth model, *Phys. Earth Planet. Inter., 25*, 297-356, 1981.

Dziewonski, A. M., and D. L. Anderson, Travel times and station corrections for *P* waves at teleseismic distances, *J. Geophys. Res., 88*, 3296-3314, 1983.

Frost, H. J., and M. F. Ashby, *Deformation Mechanism Maps*, Pergamon Press, Oxford, 1982.

Garnero, E., and D. V. Helmberger, Travel times of *S* and *SKS*: Implications for three-dimensional lower mantle structure beneath the central Pacific, *J. Geophys. Res., 98*, 8225-8241, 1993.

Garnero, E. J., and D. V. Helmberger, A very slow basal layer underlying large-scale low-velocity anomalies in the lower mantle beneath the Pacific: evidence from core phases, *Phys. Earth Planet. Inter., 91*, 161-176, 1995.

Garnero, E. J., and T. Lay, Lateral variations in lowermost mantle shear wave anisotropy beneath the north Pacific and Alaska, *J. Geophys. Res., 102*, 8121-8135, 1997.

Garnero, E. J., and T. Lay, Effects of D" anisotropy on seismic velocity models of the outermost core, *Geophys. Res. Lett.*, submitted, 1998.

Garnero, E. J., D. V. Helmberger, and S. Grand, Preliminary evidence for a lower mantle shear wave velocity discontinuity beneath the central Pacific, *Phys. Earth Planet. Inter., 79*, 335-347, 1993.

Garnero, E. J., J. Revenaugh, Q. Williams, T. Lay, and L. Kellogg, Ultra-low velocity zone at the core-mantle boundary, *This volume*, 1998.

Goarant, F., F. Guyot, J. Peyronneau, and J.-P. Poirier, High-pressure and high-temperature reactions between silicates and liquid iron alloys, in the diamond anvil cell, studied by analytical electron microscopy, *J. Geophys. Res., 97*, 4477-4487, 1992.

Grand, S. P., R. D. van der Hilst, S. Widiyantoro, Global seismic tomography: A snapshot of convection in the Earth, *GSA Today, 7*, 1-7, 1997.

Grechka, V. Y., and G. A. McMechan, Anisotropy and nonlinear polarization of body waves in exponentially heterogeneous media, *Geophys. J. Int., 123*, 959-965, 1995.

Gurnis, M., Stirring and mixing in the mantle by plate-scale flow; large persistent blobs and long tendrils coexist, *Geophys. Res. Lett., 13*, 1474-1477, 1986.

Haddon, R. A. W., Evidence for inhomogeneities near the core-mantle boundary, *Philos. Trans. R. Soc. London A, 306*, 61-70, 1982.

Hansen, U., and D. A. Yuen, Numerical simulations of thermal-chemical instabilities at the core-mantle boundary, *Nature, 334*, 237-240, 1988.

Irifune, T., Absence of an aluminous phase in the upper part of the Earth's lower mantle, *Nature, 370*, 131-133, 1994.

Irifune, T., and A. E. Ringwood, Phase transformations in primitive MORB and pyrolite compositions to 25 GPa and some geophysical implications, in *High Pressure Research in Mineral Physics,* Eds. Y. Syono and M.H. Manghnani, pp. 231-242, American Geophysical Union, Washington, D.C., 1987.

Ito, E., K. Morooka, O. Ujike and T. Katsura, Reactions between molten iron and silicate melts at high pressure: Implications for the chemical evolution of Earth's core, *J. Geophys. Res., 100*, 5901-5910, 1995.

Jackson, I., and H. Niesler, The elasticity of periclase to 3 GPa and some geophysical implications, in *High Pressure Research in Geophysics,* Eds. S. Akimoto and M. H. Manghnani, pp. 93-113, Center for Academic Publications, Tokyo, 1982.

Kaneshima, S., and P. G. Silver, A search for source-side anisotropy, *Geophys. Res. Lett., 19*, 1049-1052, 1992.

Karato, S.-I., Seismic anisotropy: mechanisms and tectonic implications, In: *Rheology of Solids and of the Earth,* edited by S. Karato and M. Toriumi, Oxford University Press, Oxford, pp. 393-422, 1989.

Karato, S.-I., Seismic anisotropy in the deep mantle, boundary layers and the geometry of mantle convection, *PAGEOPH*, in press, 1997.

Karato, S.-I., S. Zhang, and H.-R. Wenk, Superplasticity in Earth's lower mantle: Evidence from seismic anisotropy and rock physics, *Science, 270*, 458-461, 1995.

Karki, B. B., L. Stixrude, S. J. Clark, M. C. Warren, G. J. Ackland and J. Crain, Elastic properties of orthorhombic MgSiO3 perovskite at lower mantle pressures, *Am. Mineral., 82*, 635-638, 1997.

Kawasaki, I., Azimuthally anisotropic model of the oceanic upper mantle, *Phys. Earth Planet. Inter., 43*, 1-21, 1986.

Kellogg, L. H., and D. L. Turcotte, Mixing and the distribution of heterogeneities in a chaotically convecting mantle, *J. Geophys. Res., 95*, 421-432, 1990.

Kellogg, L. H., and S. D. King, Effect of mantle plumes on the growth of D" by reaction between the core and mantle, *Geophys. Res. Lett., 20*, 379-382, 1993.

Kendall, J.-M., and C. Nangini, Lateral variations in D" below the Caribbean, *Geophys. Res. Lett., 23*, 399-402, 1996.

Kendall, J.-M., and P. G. Silver, Constraints from seismic anisotropy on the nature of the lowermost mantle, *Nature, 381*, 409-412, 1996.

Kendall, J.-M., and P. G. Silver, Investigating causes of D" anisotropy, *This volume*, 1998.

Kendall, J.-M., and C. J. Thomson, Seismic modeling of subduction zones with inhomogeneity and anisotropy - 1. Teleseismic *P*-wavefront tracking, *Geophys. J. Int., 112*, 39-66, 1993.

Kesson, S., J. D. FitzGerald and J. M. G. Shelley, Mineral chemistry and density of subducted basaltic crust at lower-mantle pressures, *Nature, 372*, 767-769, 1994.

Kind, R., and G. Müller, Computations of *SV* waves in realistic Earth models, *J. Geophys., 41*, 142-172, 1975.

Kind, R., and G. Müller, The structure of the outer core from SKS amplitudes, *Bull. Seism. Soc. Am., 67*, 1541-1554, 1977.

Knittle, E. and R. Jeanloz, Synthesis and equation of state of (Mg,Fe)SiO_3 perovskite to over 100 GPa, *Science, 235*, 668-670, 1987.

Knittle, E., and R. Jeanloz, Simulating the core-mantle boundary: An experimental study of high-pressure reactions between silicates and liquid iron, *Geophys. Res. Let., 16*, 609-612, 1989.

Knittle, E., and R. Jeanloz, Earth's core-mantle boundary: Results of experiments at high pressures and temperatures, Sciences, 251, 1438-1443, 1991.

Lay, T., Structure of the core-mantle transition zone: A chemical and thermal boundary layer, *EOS Trans. AGU, 70*, 49, 54-55, 58-59, 1989.

Lay, T., Seismology of the lower mantle and core-mantle boundary, *Rev. of Geophys., Suppl.*, 325-328, 1995.

Lay, T., and D. V. Helmberger, A lower mantle *S*-wave triplication and the shear velocity structure of D", *Geophys. J. R. Astron. Soc., 75*, 799-838, 1983a.

Lay, T., and D. V. Helmberger, The shear-wave velocity gradient at the base of the mantle, *J. Geophys. Res., 88*, 8160-8170, 1983b.

Lay, T., and C. J. Young, The stably stratified outermost core revisited, *Geophys. Res. Lett.*, *17*, 2001-2004, 1990.

Lay, T., and C. J. Young, Analysis of seismic SV waves in the core's penumbra, *Geophys. Res. Lett.*, *18*, 1373-1376, 1991.

Lay, T., Q. Williams, and E. J. Garnero, The core-mantle boundary layer and deep earth dynamics, *Nature,* in press, 1998.

Lay, T., E. J. Garnero, C. J. Young, and J. B. Gaherty, Scale lengths of shear velocity heterogeneity at the base of the mantle from *S* wave differential travel times, *J. Geophys. Res.*, *102*, 9887-9909, 1997.

Li, X. D., and B. Romanowicz, Global mantle shear velocity model developed using nonlinear asymptotic coupling theory, *J. Geophys. Res.*, *101*, 22245-22272, 1996.

Lithgow-Bertelloni, C., and M. Richards, The dynamics of Cenozoic and Mesozoic plate motions, *Rev. of Geophys.*, in press, 1997.

Loper, D. E., and T. Lay, The core-mantle boundary region, *J. Geophys. Res.*, *100*, 6397-6420, 1995.

Mao, H. K., R. J. Hemley, Y. Fei, J. F. Shu, L. C. Chen, A. P. Jephcoat, Y. Wu, and W. A. Bassett, Effect of pressure, temperature, and composition on lattice parameters and density of (Fe, Mg)SiO_3-Perovskites to 30 GPa, *J. Geophys. Res.*, *96*, 8069-8079, 1991.

Matzel, E., M. K. Sen, and S. P. Grand, Evidence for anisotropy in the deep mantle beneath Alaska, *Geophys. Res. Lett.*, *23*, 2417-2420, 1996.

Maupin, V., On the possibility of anisotropy in the D" layer as inferred from the polarization of diffracted S waves, *Phys. Earth Planet. Inter.*, *87*, 1-32, 1994.

Meade, C., H. K. Mao, and J. Z. Hu, High-temperature phase transition and dissociation of (Mg,Fe)SiO_3 perovskite at lower mantle pressures, *Science, 268*, 1743-1745, 1995a.

Meade, C., P. G. Silver, and S. Kaneshima, Laboratory and seismological observations of lower mantle isotropy, *Geophys. Res. Lett.*, *22*, 1293-1296, 1995b.

Mitchell, B. J., and D. V. Helmberger, Shear velocities at the base of the mantle from observations of S and ScS, *J. Geophys. Res.*, *78*, 6009-6020, 1973.

Morris, E. M., R. W. Raitt and G. G. Shor, Velocity anisotropy and delay time maps of the mantle near Hawaii, *J. Geophys. Res.*, *74*, 4300-4316, 1969.

Nataf, H.-C., I. Nakanishi, and D. L. Anderson, Measurement of mantle wave velocities and inversion for lateral heterogeneities and anisotropy, 3. Inversion, *J. Geophys. Res.*, *91*, 7261-7307, 1986.

Nishimura, C. E. and D. W. Forsyth, Rayleigh wave phase velocities in the Pacific with implications for azimuthal anisotropy and lateral heterogeneity, *Geophys. J. Roy. Astron. Soc.*, *94*, 479-501, 1988.

Olson, P., and C. Kincaid, Experiment on the interaction of thermal convection and compositional layering at the base of the mantle, *J. Geophys. Res.*, *96*, 4347-4354, 1991.

Olson, P., G. Schubert, and C. Anderson, Plume formation in the D" layer and the roughness of the core-mantle boundary, *Nature, 327*, 409-413, 1987.

Pulliam, J., and M. K. Sen, Seismic anisotropy in the core-mantle transition zone, *Geophys. J. Int.*, in press, 1997.

Ritsema, J., E. Garnero, and T. Lay, A strongly negative shear velocity gradient and lateral variability in the lowermost mantle beneath the Pacific, *J. Geophys. Res.*, *102*, 20,395-20,411, 1997.

Ritsema, J., T. Lay, E. J. Garnero, and H. Benz, Seismic anisotropy in the lowermost mantle beneath the Pacific, *Geophys. Res. Lett.*, in press, 1998.

Russell, S., T. Lay, and E. J. Garnero, Small-scale boundary layer structure in the lowermost mantle: Evidence for inflow at the root of the Hawaiian plume, *Nature*, in press, 1998.

Saxena, S.K. et al., Stability of perovskite ($MgSiO_3$) in the Earth's mantle, *Science, 274*, 1357-1359, 1996.

Schweitzer, J., and G. Müller, Anomalous difference traveltimes and amplitude ratios of *SKS* and *SKKS* from Tonga-Fiji events, *Geophys. Res. Lett.*, *13*, 1529-1532, 1986.

Silver, P. G., Seismic anisotropy beneath the continents: Probing the depths of geology, *Annu. Rev. Earth Planet. Sci.*, *24*, 385-432, 1996.

Sleep, N. H., Gradual entrainment of a chemical layer at the base of the mantle by overlying convection, *Geophys. J.*, *95*, 437-447, 1988.

Song, Y., and T.J. Ahrens, Pressure-temperature range of reactions between liquid iron in the outer core and mantle silicates, *Geophys. Res. Lett.*, *21*, 153-156, 1994.

Stacey, F. D., and D. E. Loper, The thermal boundary layer interpretation of D" and its role as a plume source, *Phys. Earth Planet. Inter.*, *33*, 45-55, 1983.

Stixrude, L., R. E. Cohen, R. Yu and H. Krakauer, *Am. Mineral.*, *81*, 1293-1296, 1996.

Su, W-J., R. Woodward, and A.M. Dziewonski, Degree 12 model of shear velocity heterogeneity in the mantle, *J. Geophys. Res.*, *99*, 6945-6980, 1994.

Tackley, P. J., On the penetration of an endothermic phase transition by upwellings and downwellings, *J. Geophys. Res.*, *100*, 15,477-15,488, 1995.

Tanimoto, T., and D. L. Anderson, Lateral heterogeneity and azimuthal anisotropy of the upper mantle: Love and Rayleigh waves 100-250 s, *J. Geophys. Res.*, *90*, 1842-1858, 1985.

Valenzuela, R., and M. E. Wysession, The base of the mantle as illuminated by core-diffracted waves, *This volume*, 1998.

Vassiliou, M. S. and T. J. Ahrens, The equation of state of $Mg_{0.6}Fe_{0.4}O$ to 200 GPa, *Geophys. Res. Lett.*, *9*, 127-130, 1982.

Vidale, J. E., and H. M. Benz, Seismological mapping of fine structure near the base of Earth's mantle, *Nature, 361*, 529-532, 1993.

Vinnik, L., L. Breger, and B. Romanowicz, Anisotropic structures at the base of the oceanic mantle, *Nature*, in press, 1998.

Vinnik, L. P., V. Farra, and B. Romanowicz, Observational evidence for diffracted SV in the shadow of the Earth's core, *Geophys. Res. Lett.*, *16*, 519-522, 1989.

Vinnik, L., B. Romanowicz, Y. Le Stunff, and L. Makeyeva, Seismic anisotropy in the D" layer, *Geophys. Res. Lett.*, *22*, 1657-1660, 1995.

Weber, M., Lamellae in D"? An alternative model for lower mantle anomalies, *Geophys. Res. Lett., 21*, 2531-2534, 1994.

Weidner, D. J., J. D. Bass, A. E. Ringwood and W. Sinclair, The single-crystal elastic moduli of stishovite, *J. Geophys. Res., 87*, 4740-4746, 1982.

Wessel, P., and W. H. F. Smith, Free software helps map and display data, *EOS, 72*, 441, 445-446, 1991.

Williams, Q.,The temperture contrast across D", *This volume*, 1998.

Williams, Q., and E. J. Garnero, On the possible origin of a seismically thin boundary layer at the base of the mantle, *Science, 273*, 1528-1530, 1996.

Williams, Q., and R. Jeanloz, Melting relations in the iron-sulfur system at high pressures: Implications for the thermal state of the Earth, *J. Geophys. Res., 95*, 19299-19310, 1990.

Winchester, J. P., and K. C. Creager, Azimuthal anisotropy and abrupt transitions from slow to fast anomalies in the velocity structure of D", *Proc. of 1997 IRIS Meeting*, abstract.

Wysession, M. E., Continents of the core, *Nature, 381*, 373-374, 1996.

Wysession, M. E., T. Lay, E. J. Garnero, J. Revenaugh, Q. Williams, D. V. Helmberger, R. Jeanloz, and L. Kellogg, Large-scale structure of D": Lateral gradients and discontinuity variations, *This volume*, 1998.

Yeganeh-Haeri, Y., Synthesis and re-investigation of the elastic properties of single-crystal magnesium silicate perovskite, *Phys. Earth Planet. Inter., 87*, 111-121, 1994.

Young, C. J., and T. Lay, The core-mantle boundary, *Annu. Rev. Earth Planet. Sci., 15*, 25-46, 1987.

Young, C. J., and T. Lay, The core shadow zone boundary and lateral variations of the P velocity structure of the lowermost mantle, *Phys. Earth Planet. Int., 54*, 64-81, 1989.

Young, C. J., and T. Lay, Multiple phase analysis of the shear velocity structure in the D" region beneath Alaska, *J. Geophys. Res., 95*, 17385-17402, 1990.

Edward J. Garnero, Department of Geology and Geophysics, University of California, Berkeley, CA 94720.

Louise Kellogg, Department of Geology, University of California, Davis, CA 95616.

Thorne Lay, Earth Sciences Department, University of California, Santa Cruz, CA 96064.

Quentin Williams, Earth Sciences Department, University of California, Santa Cruz, CA 95064.

Michael E. Wysession, Department of Earth and Planetary Sciences, Washington University, St. Louis, MO, 63130.